

OVERVIEW AND STATUS OF BEAM DIAGNOSTICS FOR THE INJECTOR LINAC OF THE SIAM PHOTON SOURCE

P. Boonpornprasert, T. Chanwattana*, S. Bootiew, S. Chunjarean,
C. Dhammatong, N. Juntong, T. Pulampong, S. Klinkhieo
Synchrotron Light Research Institute, Nakhon Ratchasima, Thailand

Abstract

The Synchrotron Light Research Institute (SLRI) operates the Siam Photon Source (SPS) in Nakhon Ratchasima, Thailand. The primary injector for this facility is a linear accelerator (linac) that accelerates electron bunches to 40 MeV. The beam is then guided to a booster ring via the Low-Energy Beam Transport (LBT) line. To ensure the delivery of a high-quality beam for injection, a set of diagnostic instruments is used to monitor the beam properties. This paper presents the current status of the beam instrumentation for the SPS injector linac, providing an overview of the systems used to measure the beam current, transverse profiles, and energy. The latest measurement results show an overall transmission efficiency of 25.6 % and indicate that the beam energy is approximately 10 % lower than the nominal value. These findings provide a new baseline for the future optimization of the injector system.

INTRODUCTION

The Synchrotron Light Research Institute (SLRI), located in Nakhon Ratchasima, Thailand, operates the 1.2 GeV Siam Photon Source (SPS). For many years, the facility has provided synchrotron light to a community of academic and industrial users [1]. In parallel with the design and planning phase for a new 3 GeV, 4th generation light source, the Siam Photon Source II (SPS-II) [2], the continued improvement and the maintenance of a high-performance operation for the existing SPS facility remain a high priority.

The SPS consists of an injector linac, a booster synchrotron, and a storage ring. The facility was established with components from the former SORTEC facility in Japan [3]. During the reassembly in Thailand, the original designs of the linac and the booster remained unchanged, while the High-Energy Beam Transport line (HBT) and the storage ring were modified [4]. The design and performance of the linac, which can generate and accelerate an electron beam to 40 MeV, are reported in [5]. The beam is then transported to the booster ring through the Low-Energy Beam Transport line (LBT). The properties of this electron beam determine the injection efficiency into the booster. Consequently, diagnostic instruments are installed in the beamline to monitor and optimize the beam, ensuring its high quality and efficient transport.

To ensure reliable monitoring and optimization, the beam diagnostics of the SPS injector linac have recently been upgraded [6]. This paper provides an overview of the current instrumentation for the linac and the LBT. Furthermore,

recent measurement results are presented, which provide an updated performance baseline for the ongoing improvement of the SPS injector system.

LINAC SYSTEM DESCRIPTION

A schematic layout of the SPS injector linac and LBT is shown in Fig. 1. The electron beam is generated and accelerated to 40 MeV by a series of components. The main subsystems are described below, with operational parameters listed in Table 1.

Electron Source

The electron beam is generated from a triode-type thermionic DC gun, which uses a cathode manufactured by EIMAC (Y646B), a control grid, and an anode to generate the initial beam. The gun operates with an accelerating high voltage of 100 kV. A grid pulser supplies a voltage pulse with a duration of 3 μ s at a repetition rate of 0.3 Hz to produce the electron beam.

Bunching System

Following the gun, the beam enters a bunching system designed to longitudinally compress the beam. The system consists of two single-gap pre-buncher cavities (PB1 and PB2) and a main buncher, all operating at a resonant frequency of 2856 MHz. The main buncher is a 8.5-cell standing-wave side-coupling structure.

Accelerating Structures

The main acceleration is provided by two S-band (2856 MHz) traveling-wave structures. Each structure is 2.3 m long and operates in the $2\pi/3$ mode with a constant-gradient design. The two structures, operating in series, accelerate the electron beam to its final energy of 40 MeV.

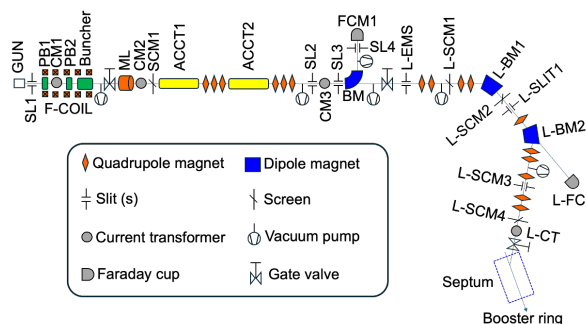


Figure 1: Layout of the SPS injector linac injector and LBT.

* Corresponding Author, thakonwat@slri.or.th

Table 1: Operational Parameters of the SPS Injector Linac

Parameter	Value
Gun accelerating HV	100 kV
Gun grid pulse voltage	92 V
Gun grid bias voltage	-33.7 V
RF operating frequency	2856 MHz
RF macropulse width	3 μ s
Repetition rate	0.3 Hz
RF input power (for each pre-buncher)	1.4 kW
RF input power (for buncher)	3.4 MW
Klystron RF output power (for both linacs)	20 MW

BEAM INSTRUMENTATION

The linac and LBT are equipped with several diagnostic devices to measure the beam parameters.

Beam Current Monitors

Four monitors are installed along the linac and LBT to measure the beam current and charge, as shown in Fig. 1.

- CM1 and CM2 are wall current monitors (WCMs) located after the pre-buncher PB1 and after the buncher, respectively.
- CM3 is an AC Current Transformer (ACCT) manufactured by Bergoz Instrumentation, which replaced the original WCM at the exit of the linac in November 2022 [6].
- L-CT is a Pearson Electronics Model 3100 current transformer, located at the end of LBT.

The signals from these monitors are sent to an oscilloscope in the control room for data acquisition. In addition, two Faraday cups (FCM1 and L-FC) are present in the beamline but have been disabled for many years and are not used in routine operations.

Transverse Profile Monitors

Several monitoring screens are installed in the beamline to measure the transverse beam profile, as shown in Fig. 1. Each monitor uses a movable scintillating screen that is inserted into the beam path at a 45° angle. The light produced by the beam interaction is captured by a CCD camera to form an image of the profile. The original system was unreliable due to radiation damage to the cameras. To improve reliability, the system was upgraded by adding a mirror to the optical path. This mirror directs the light vertically, allowing the camera to be placed farther from the primary radiation plane. The details and the current status of this upgrade are reported in [6, 7].

Beam Energy Measurement

There are three bending magnets in the beamline: BM, L-BM1, and L-BM2.

The first magnet, BM, is a dipole with a bending angle of 90°, located after the accelerating structure ACCT2. It has a bending radius of 402.5 mm. For a 40 MeV beam, the required magnetic field is 0.3357 T, which corresponds to an applied current of 18.89 A. Downstream from this magnet, a slit (SL4) and a Faraday cup (FCM1) can be used to measure the beam energy spectrum.

The L-BM1 and L-BM2 magnets are identical dipoles that each have a bending angle of 50.5° and a bending radius of 500 mm. To guide a 40 MeV beam, a magnetic field of 0.2702 T is required, corresponding to an applied current of 12.86 A. The L-BM1 magnet, when used with the screen monitor SCM2, serves as a spectrometer to measure the beam energy profile.

LATEST MEASUREMENT RESULTS

The SPS facility provides about 3,000 to 4,000 hours of beam time for users annually, with injection to the storage ring typically performed twice a day [1, 8]. During these routine injections, the performance of the linac is monitored using signals from the current monitors (CM1, CM2, CM3) and the current transformer (L-CT). While these checks are sufficient for daily operation, a detailed measurement and analysis of the beam current and transmission efficiency is performed every several years to establish a performance benchmark. The results from the latest of these measurements are presented in this section.

Beam Current and Transmission

The latest beam current measurements were performed in June 2025 under normal operating conditions. The waveform data from each current monitor was acquired from an oscilloscope and analyzed offline. The analysis procedure includes a baseline correction to the raw voltage signal, a conversion to current using the respective calibration factors, and numerical integration over the pulse to calculate the total beam charge. The resulting current waveforms and their calculated charges are shown in Fig. 2.

The results from the latest measurements are compared with historical data from 2006 [9] and 2016 [10] in Fig. 3. The top plot shows the absolute charge measured at each of the four current monitors, while the bottom plot shows the calculated stage-to-stage transmission efficiency between consecutive monitors. The transmission from the linac exit to the end of the LBT (L-CT vs CM3) has increased to 57.8 %, a notable recovery from the 37.6 % measured in 2016.

The results from the latest measurements are compared with historical data from 2006 and 2016 [9, 10] in Fig. 3. The top plot shows the absolute charge at each monitor, while the bottom plot shows both the stage-to-stage and overall transmission efficiencies. The most recent data indicates that the transmission from the linac exit to the end of the LBT (L-CT vs CM3) has increased to 57.8 %, a notable recovery from the 37.6 % measured in 2016. The overall transmission

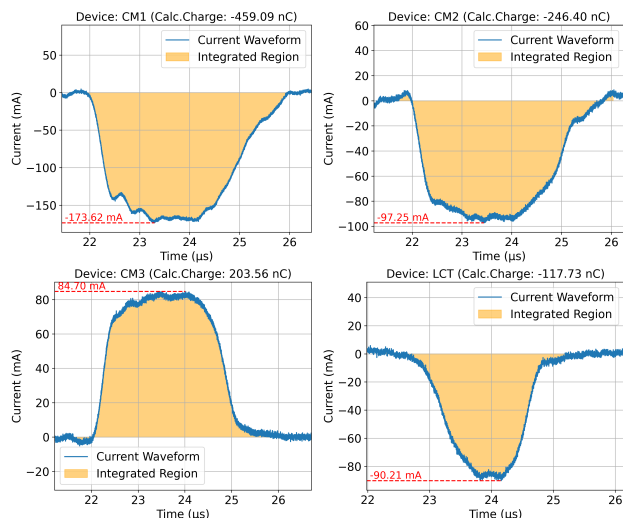


Figure 2: Current waveforms measured at CM1, CM2, CM3, and L-CT. The shaded area indicates the region used for charge integration, and the calculated total charge is shown for each monitor.

from the PB1 exit to the end of the LBT (L-CT vs CM1) is now 25.6 %.

A point of concern is the transmission from the linac exit (CM3) to the LBT (L-CT), which remains below 60 %. In principle, the transmission in this section should be close to 100 % because it contains only drift spaces and static magnetic fields, with no accelerating cavities or collimators that would cause significant beam loss. This is the point that we plan to investigate and improve in the future.

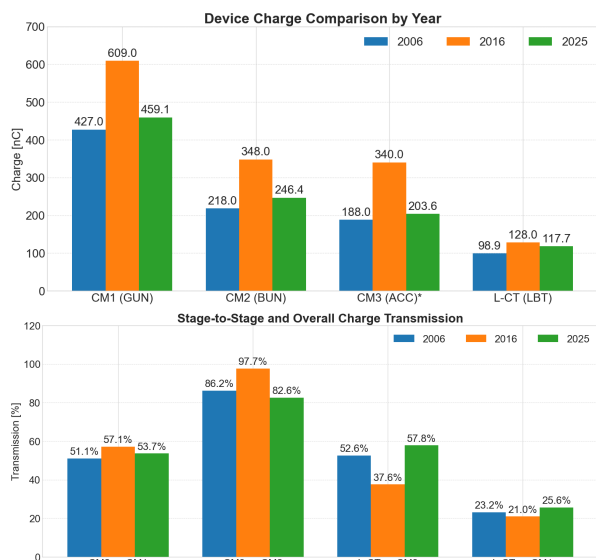


Figure 3: Comparison of beam charge measurements from 2006, 2016, and 2025. Top: Absolute beam charge measured at each current monitor. Bottom: Stage-to-stage transmission efficiency between consecutive monitors and the overall transmission from the PB1 exit to the end of the LBT (L-CT vs CM1).

Beam Energy Estimation

The recent measurements have focused primarily on beam current, as detailed measurements of transverse profiles have not been performed for several years. Future studies are planned for measurements of the transverse emittance and the energy profile. However, a preliminary analysis of the beam energy was made using the operational settings of the L-BM1 magnet. With an applied current of 11.26 A, corresponding to a magnetic field of 0.237 T, the average beam energy was calculated from the magnetic rigidity to be approximately 35.47 MeV. This value is about 10 % lower than the nominal energy of 40 MeV.

SUMMARY AND OUTLOOK

The current status of beam instrumentation at the SPS injector linac and LBT is presented, along with the latest measurement results. The overall beam transmission efficiency from the PB1 exit to the end of the LBT was measured to be 25.6 %. While this is a slight improvement over previous years, significant beam loss is still observed in the LBT section. A preliminary analysis of the beam energy, based on magnet settings, suggests the energy is approximately 10 % lower than the nominal energy of 40 MeV. These results provide a new baseline for future improvements to the injector system.

Future work will focus on improving the transmission efficiency through the LBT. This will involve detailed beam dynamics simulations and experimental studies. The screen monitors will be used to perform measurements of the transverse beam profile and emittance. Furthermore, the energy and energy spread will be measured to verify the operational energy of the injector linac.

ACKNOWLEDGEMENTS

This work was supported by the Synchrotron Light Research Institute (SLRI), Thailand Science Research and Innovation (TSRI), and the National Science, Research and Innovation Fund (NSRF) (NRIIS number 4824056). The authors thank the SLRI SPS operation team for their support and acknowledge the use of AI writing assistants, including Google Gemini and ChatGPT, to improve the language and clarity of this report. All content and any potential errors remain the responsibility of the authors.

REFERENCES

- [1] N. Juntong *et al.*, “Seven years statistical analysis of the Siam photon source operation”, in *Proc. IPAC’23*, Venice, Italy, May 2023, paper MOPM027, pp. 1042–1045. doi: 10.18429/JACoW-IPAC2023-MOPM027
- [2] P. Klysubun *et al.*, “SPS-II: A 4th Generation Synchrotron Light Source in Southeast Asia”, in *Proc. IPAC’22*, Bangkok, Thailand, Jun. 2022, paper MOPOTK034, pp. 764–768. doi: 10.18429/JACoW-IPAC2022-MOPOTK034
- [3] M. Kodaira *et al.*, “Development of Highly Stable Synchrotron Radiation Source at SORTEC”, *Jpn. J. Appl. Phys.*,

- vol. 30, no. 11S, p. 3043, Nov. 1991.
doi:10.1143/JJAP.30.3043
- [4] W. Pairsuwan and T. Ishii, “The Siam Photon Laboratory”, *J. Synchrotron Rad.*, vol. 5, pp. 1173-1175, May 1998.
doi:10.1107/S0909049597018335
- [5] M. Shiota *et al.*, “Design and Performance of the 40 MeV Linac and Beam Transport System for the 1 GeV Synchrotron Radiation Source at SORTEC”, in *Proc. the 2nd International Symposium on Advanced Nuclear Energy Research*, Osaka, Japan, May 1990, pp. 302–305.
- [6] T. Chanwattana *et al.*, “Upgrades of beam diagnostics for linac of Siam Photon Source”, in *Proc. IPAC’23*, Venice, Italy, May 2023, paper MOPM028, pp. 1046–1049.
doi:10.18429/JACoW-IPAC2023-MOPM028
- [7] T. Chanwattana *et al.*, “Upgrade of Screen Monitor System for the Injector Linac of the Siam Photon Source”, presented at IBIC’25, Liverpool, UK, Sep. 2025, paper TUPMO29, this conference.
- [8] S. Suebka *et al.*, “Optimization of Siam Photon Source storage ring using Badger”, presented at the IPAC’25, Taipei, Taiwan, Jun. 2025, paper THPM100, pp. 2898–2900.
doi:10.18429/JACoW-IPAC25-THPM100
- [9] S. Cheedket *et al.*, “The efficiency of the SPS injection system”, SLRI, Nakhon Ratchasima, Thailand, Rep. NSRC-TN-2006/06, Sep. 2006.
- [10] S. Kongtawong *et al.*, “A new injection efficiency measurement system for the Siam Photon Source”, SLRI, Nakhon Ratchasima, Thailand, Rep. SLRI-TN-2022-080, May 2016.